ISSN 1063-7745, Crystallography Reports, 2006, Vol. 51, No. 5, pp. 729–733. © Pleiades Publishing, Inc., 2006.
Original Russian Text © A.E. Blagov, M.V. Kovalchuk, V.G. Kohn, Yu.V. Pisarevsky, 2006, published in Kristallografiya, 2006, Vol. 51, No. 5, pp. 779–784.

DIFFRACTION AND SCATTERING OF IONIZING RADIATIONS

Dedicated to the 65th Birthday of Professor G. Fuss

Dynamic Variation in the Lattice Parameter of a Crystal under Ultrasonic Treatment in X-ray Diffraction Experiments

A. E. Blagov[a], M. V. Kovalchuk[a, b], V. G. Kohn[b], and Yu. V. Pisarevsky[a]

[a] *Shubnikov Institute of Crystallography, Russian Academy of Sciences, Leninskiĭ pr. 59, Moscow, 119333 Russia*
e-mail: aopt@ns.crys.ras.ru

[b] *Russian Research Centre Kurchatov Institute, pl. Akademika Kurchatova 1, Moscow, 123182 Russia*

Received May 15, 2006

Abstract—The X-ray diffraction in the Laue geometry is investigated in germanium and silicon single crystals upon excitation of long-wavelength ultrasonic elastic strain waves traveling along the sample surface. The X-ray diffraction beam is bounded by a slit 0.2 mm in size, which is considerably less than the wavelength of the ultrasonic wave. The use of this slit makes it possible to separate crystal regions with a nearly homogeneous strain. As a consequence, the rocking curves stroboscopically measured in a double-crystal dispersionless scheme at different instants of time almost coincide with those for a perfect crystal with a lattice parameter varying in time. The rocking curves measured in a time-integrated mode turn out to be broadened, but their integrated intensities remain unchanged. Possible applications of the developed method are discussed.

PACS numbers: 61.10.Nz

DOI: 10.1134/S1063774506050026

1. INTRODUCTION

Data on X-ray diffraction in single crystals subjected to ultrasonic elastic strain make it possible to determine a variation that occurs in the lattice parameter in different crystal regions due to the deformation. Over the past decades, a large number of works have been devoted to investigation into different aspects of this problem. One of the directions of these investigations is associated with the possibility of obtaining information on the elastic vibrations in a single crystal. This information is important for physical acoustics and can be used for controlling the quality of different piezoelectric and acoustoelectronic devices. Another direction lies in the search for new effects and fundamental features of X-ray acoustic interaction in single crystals. In particular, the use of X-ray diffraction in the Laue geometry and ultrasonic waves propagating in the direction normal to the crystal surface made it possible to reveal the resonance suppression of anomalous transmission (the Borrmann effect) at an ultrasonic wavelength equal to the extinction length [1], as well as the switching of an X-ray beam from the transmission direction to the reflection direction [2] at an ultrasonic wavelength equal to twice the crystal thickness.

In the case of diffraction in the Bragg geometry, ultrasonic treatment, as a rule, leads to excitation of surface acoustic waves, so that a large number of wavelengths correspond to the size of the crystal region exposed to the X-ray beam (see, for example, [3] and references therein). Under these conditions, in the crystal, there arises a superlattice responsible for both the appearance of additional X-ray reflection maxima (satellites) and the decrease in the intensity of the principal reflection maximum. This phenomenon can be used as an electronic analogue of a mechanical beam chopper. Other applications are based on the broadening of the rocking curve and the use of the stroboscopic technique for exciting ultrasonic waves normal to the surface of the crystal (see, for example, [4] and references therein).

In our earlier work [5], we studied a new case, namely, X-ray diffraction in the Laue geometry in a germanium single crystal upon excitation of a long-wavelength ultrasonic wave along the surface of the sample. The incident beam was bound by a slit whose size was considerably less than the wavelength of the ultrasonic strain wave. It was found that the crystal undergoes a strong strain due to the spurious vibrations. Moreover, it was revealed that static and dynamic strains are compensated for in the region where the sample and the ultrasound source are cemented together.

In this work, we experimentally investigated X-ray diffraction in germanium and silicon crystals in the case where strain of the crystal across the beam width

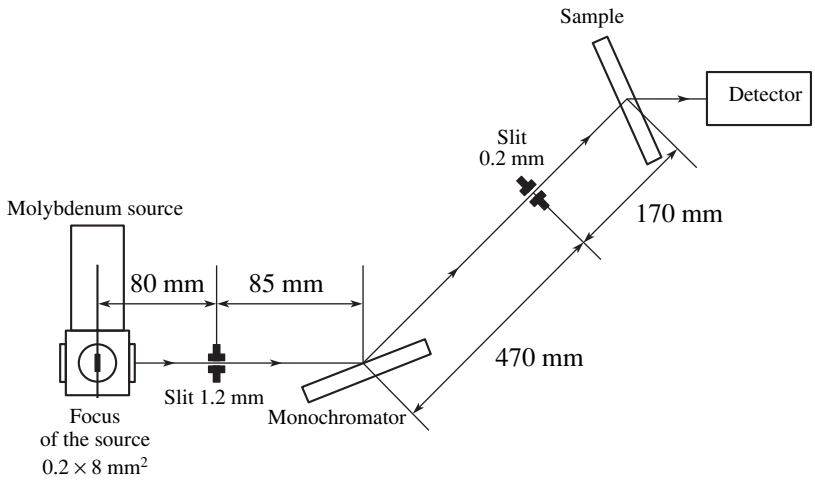

Fig. 1. X-ray optical scheme of the experiment.

appears to be virtually homogeneous in particular regions along the crystal surface or has a small gradient in other regions.

2. DESCRIPTION OF THE EXPERIMENT

The schematic diagram of the experimental setup assembled on the basis of a TRS-1 X-ray diffractometer [6] is depicted in Fig. 1. The experiments were carried out with germanium and silicon crystals in the double-crystal dispersionless diffraction scheme. The monochromator and the sample were the plates with the [110] and $[1\bar{1}1]$ surface orientations. The measurements were performed in a (220) symmetric diffraction geometry for both the monochromator and the sample, but the monochromator was set in the Bragg geometry, whereas the sample was set in the Laue geometry. The X-ray tube had a molybdenum anode, and the focal spot size was 0.2×8 mm^2. A slit separating the Mo$K_{\alpha 1}$ spectral line was located ahead of the sample. The spatially integrated intensity of the diffracted beam was measured with a scintillation detector.

Ultrasonic vibrations in the crystal under investigation (sample) were excited with a piezoelectric crystal transducer, in which longitudinal vibrations along the length of the plate were induced by the electromagnetic signal fed to the lateral surfaces from a high-frequency generator. The surfaces were coated with conducting platinum layers deposited by cathode sputtering. The piezoelectric crystal transducer was prepared from a (*XY*twl, –18.5°/0°/0°)-cut quartz crystal. The piezoelectric crystal transducer and the crystal under investigation were cemented together by their ends and represented a composite resonator. In order to ensure the vibrational purity and the vibrational quality, the widths of the sample and piezoelectric crystal transducer plates were several times less than their lengths and the plate ends were polished.

The condition providing mechanical resonance in the "piezoelectric crystal transducer–sample" system is the coincidence of their resonant frequencies. Under this condition, there arise high-quality vibrations and a bulk longitudinal standing wave. In this case, one-half of the wavelength of the fundamental elastic wave with the maximum strain at the center of the sample and the nodes at the boundaries falls on each plate. The sample length was many times larger than the size of the crystal region exposed to the X-ray beam, and the length of the piezoelectric crystal transducer was chosen so that the natural frequencies of the sample and the piezoelectric crystal transducer coincided with each other. The calculated natural frequency of the sample was equal to 126.5 kHz. The piezoelectric crystal transducer was tuned to this frequency. Since the amplitude depended strongly on the vibrational frequency, a high-stability signal generator was used and the tuning to resonance was controlled against a special high-frequency voltmeter.

The ultrasonic generation system was supplemented by an electronic circuit that provided a way of performing the stroboscopic measurements. A pulse generator produced pulses with a controlled shift in phase of vibrations of the piezoelectric crystal transducer (the error in the adjustment was no more than 10%). A coincidence circuit for each pulse allowed diffracted photons to be counted. The time interval of counting was equal to one-tenth of the period of vibrations of the piezoelectric crystal transducer. This permitted us to record the diffracted beam under conditions of quasi-static strain pertaining to a specific phase of vibrations of the crystal under investigation.

3. RESULTS OF THE EXPERIMENT

Germanium

The germanium crystal measured $19.5 \times 10 \times 0.4$ mm^3 along the x, y, and z axes, respectively. The

sound propagated along the x axis. The crystal thickness t (along the z axis) corresponded to the Borrmann effect with the absorption factor $\mu t \approx 12$ (where μ is the linear absorption coefficient). The rocking curves were measured upon small rotation of the sample with respect to the exact Bragg position specified by the monochromator crystal. Figure 2 shows the rocking curves measured in a time-integrated mode at different ultrasonic powers in the crystal region with almost homogeneous strain across the beam width. The germanium crystal had a high quality. This can be judged from the half-width of the rocking curve measured without ultrasound: the half-width is equal to 6″, which is close to the theoretical value for a perfect crystal. The errors in the measurement of the angle and intensity were less than 0.5 and 1.0%, respectively.

As the vibrational amplitude (ultrasonic power) increases, the rocking curve is broadened in a nearly symmetric fashion. However, the area under the curve remains unchanged to within the accuracy of the measurements. Therefore, the total number of reflected photons remains constant, but they are distributed over a wider angular range. This corresponds to the situation when, at different instants of time, scattering occurs incoherently from the crystal lattice with the lattice parameter (and, accordingly, the Bragg angle) varying with time. A decrease in the intensity with a broadening of the rocking curve is associated with the fact that the crystal spends a shorter time in each strain state.

The rocking curves measured using the stroboscopic technique described above at different φ phases of vibrations are depicted in Fig. 3. It can be seen from this figure that the rocking curves pertaining to the phases $\varphi = -\pi/2$ and $\pi/2$ are shifted with respect to the central curve by –20″ and +20″, respectively. This means that, at the corresponding instants of time, the lattice parameter changes almost uniformly across the width of the crystal region exposed to the X-ray beam. However, the strain is slightly inhomogeneous, because the curves are somewhat broadened and have a slightly asymmetric shape.

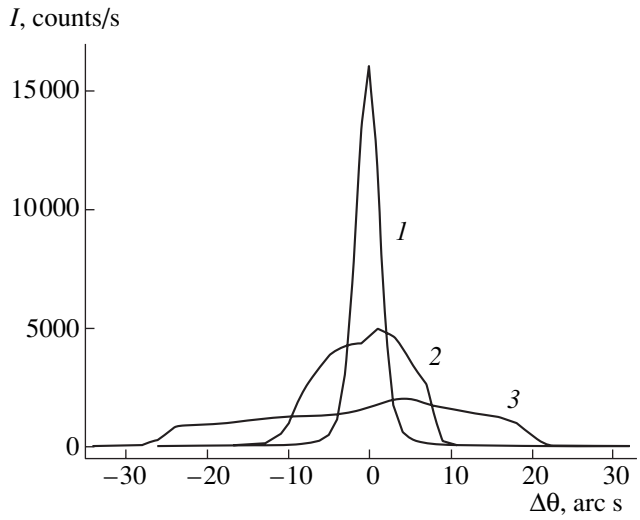

Fig. 2. Rocking curves measured in a time-integrated mode for Ge(220) at different ultrasonic powers: (*1*) without sound, (*2*) 40% of the maximum ultrasonic power, and (*3*) the maximum ultrasonic power (0.1 W).

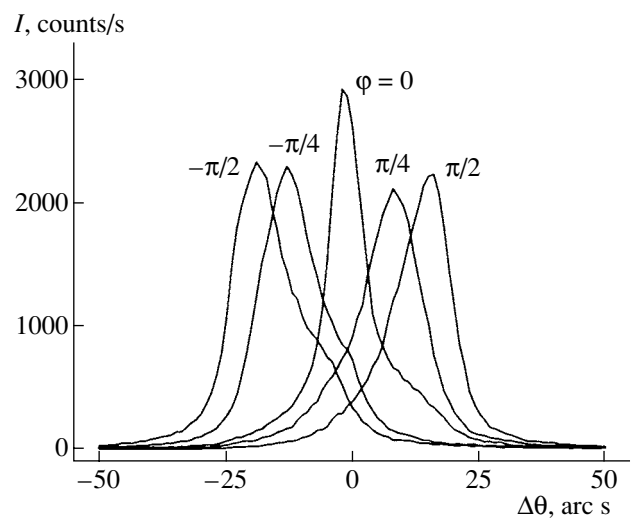

Fig. 3. Rocking curves stroboscopically measured for Ge(220) at different φ phases of vibrations of the acoustic resonator.

Silicon

The silicon crystal measured $30 \times 10 \times 0.9$ mm^3 along the x, y, and z axes, respectively. The sound propagated along the x axis. The crystal thickness t (along the z axis) was larger than that of the germanium crystal but did not correspond to the Borrmann effect ($\mu t \approx 1.5$). In the given case, the vibrations are similar in character to the calculated vibrations when one-half of the wavelength of the standing wave falls on each plate. This can be judged from the measurements of the half-width θ_0 of the rocking curve in a time-integrated mode in different regions of the crystal with respect to the slit bounding the X-ray beam. The dependence of the half-width of the rocking curves on the slit position is plotted in Fig. 4. It can be seen from this figure that, although there exists a spurious short-wavelength harmonic, its amplitude is smaller than the amplitude of the fundamental harmonic.

In the crystal, it is possible to separate three regions *1*, *2*, and *3*, in which the strain either slightly linearly increases (region *1*), weakly linearly decreases (region *2*), or remains virtually constant (region *3*) with a change in the coordinate x. The rocking curves measured using the stroboscopic technique at different phases of vibrations $\varphi = -\pi/2$, 0, and $\pi/2$ in region *3* are shown in Fig. 5. As can be seen from this figure, all the rocking

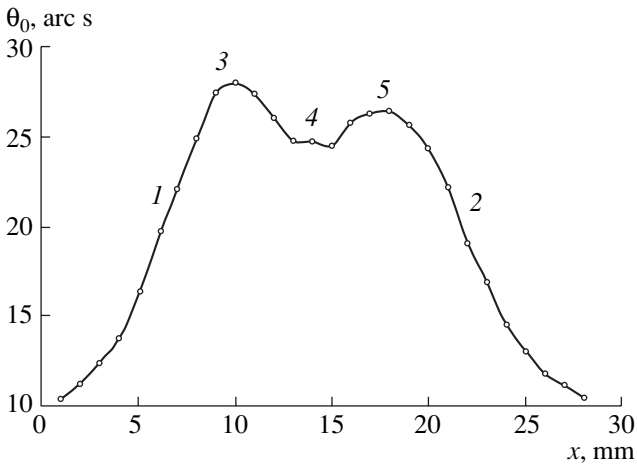

Fig. 4. Dependences of the half-width of the rocking curves measured in a time-integrated mode for Si(220) on the coordinate of the center of the slit bounding the X-ray beam along the surface of the sample.

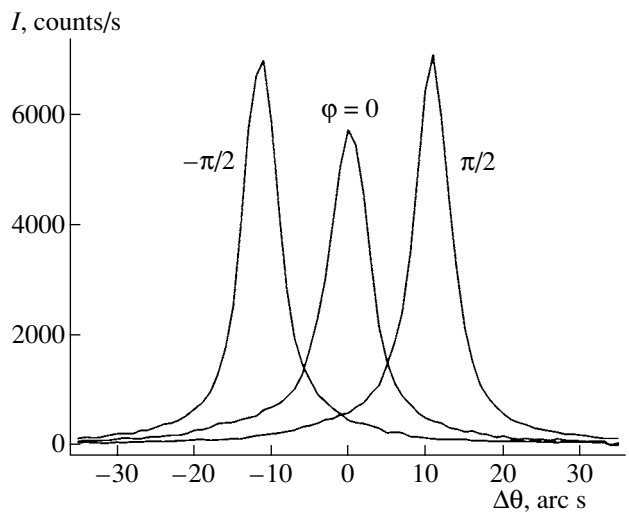

Fig. 5. Rocking curves stroboscopically measured for Si(220) at different φ phases of vibrations of the acoustic resonator in region *3* (Fig. 4) with a nearly homogeneous strain.

curves are nearly ideal in shape. Note that, compared to the side curves, the central curve is slightly broadened, its maximum intensity is lower, and the area under the curve is smaller. This is associated with the finite time interval of photon counting and the sinusoidal variation in the strain with time. The time derivative of the strain is equal to zero at the maximum strain and reaches a maximum at zero strain. Correspondingly, the strain for the central curve varies more rapidly within the time interval of the photon counting. The measurements performed in a time-integrated mode give an envelope of the curves shown in Fig. 5. Note that the aforementioned properties of the rocking curves were not observed for the germanium crystal because of the strain inhomogeneity within the width of the slit bounding the X-ray beam.

Figure 6 depicts the rocking curves stroboscopically measured in region *1* for the same phases of vibrations as in Fig. 5. The rocking curves exhibit a weakly asymmetric behavior. The number of photons in the time interval corresponding to compression of the crystal lattice is larger than that upon its tension. The rocking curve measured in a time-integrated mode is also asymmetric in shape. In region *2*, the gradient is opposite in sign and the asymmetric behavior of the curves becomes reverse. In this case, a larger number of photons are reflected in the time interval corresponding to tension of the crystal lattice. The rocking curve measured in a time-integrated mode is also characterized by opposite asymmetry.

However, the half-widths of the rocking curves at different instants of time are close to the half-width of the rocking curve for the ideal crystal. This implies that the space change in the strain across the crystal region equal to the slit width bounding the X-ray beam is very small and, hence, virtually does not affect the shape of the rocking curve.

4. DISCUSSION OF THE RESULTS

The experimental rocking curves stroboscopically measured at different instants of time are similar to the theoretical curves obtained as a result of convolution of the angular dependence of the reflection of plane waves from the monochromator and sample crystals in the case when the lattice parameter varies according to a sinusoidal law with time and is spatially homogeneous. However, the sample is characterized by the inhomogeneous strain along the surface (almost perpendicular to the beam). Moreover, the incident beam is bounded by the slit. It is evident that the plane-wave approximation is valid if the actual width of the coherent beam is less than the slit width.

The sources of coherent radiation are atoms (points) on the surface of the anode of the X-ray tube. They emit a spherical wave, and only the monochromatic components of this wave are coherent. The spherical wave after reflection from the monochromator transforms into a narrow beam, because the monochromator has a constrained angular region of reflection. With the use of the Stepanov program [7], it is easy to find that, for the experimental conditions and the germanium monochromator, the angular width of the reflection region is $\Delta\theta = 27$ μrad. In this case, the size of the coherent beam at a distance of 63.5 cm from the source (i.e., in the region of the slit) is equal to 0.02 mm, which is ten times smaller than the slit size. Therefore, the slit does not bound the coherent beam and, hence, the plane-wave approximation holds true. In the case of the silicon monochromator, the beam width is equal to 0.008 mm and the necessary conditions are satisfied with a safety margin.

The crystal lattice of the sample can be treated as locally homogeneous when the lattice parameter in the

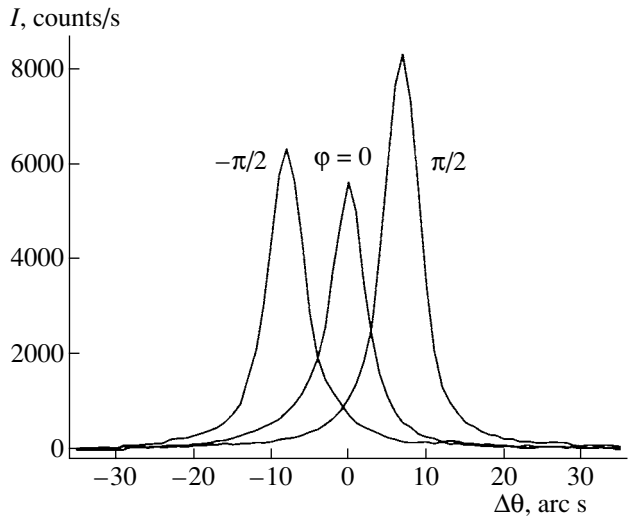

Fig. 6. Rocking curves stroboscopically measured for Si(220) at different φ phases of vibrations of the acoustic resonator in region *1* (Fig. 4) with a strain gradient.

region exposed to the X-ray beam varies insignificantly. The total region exposed to a narrow beam incident on the crystal is determined by a Borrmann fan with the longitudinal size on the exit surface of the crystal $\Delta = 2t\tan\theta_B$. For the germanium sample ($t = 0.4$ mm, $\theta_B = 10.2°$), we obtain the estimate $\Delta = 0.15$ mm. This size is comparable to the slit size and exceeds the size of the homogeneous-strain region in gradient regions. However, the Borrmann effect observed in the germanium sample leads to a decrease in the effective transverse size of the illuminated region in the sample, because the energy flux predominantly propagates along the normal to the crystal surface. For the silicon sample ($t = 0.9$ mm, $\theta_B = 10.6°$), we have the estimate $\Delta = 0.34$ mm. Although the size of the illuminated region in the silicon crystal is larger than that in the germanium sample, the strain in the silicon sample is smoother because the spurious harmonics make a smaller contribution (see Fig. 4). As a consequence, the aforementioned conditions are also satisfied.

The incoherent illumination of the sample is determined by the source size (0.2 mm) and the width of the Bragg angle distribution due to the finite width of the Mo$K_{\alpha 1}$ spectral line. It is known from the Du Mond diagram that $\Delta\theta_B = (\Delta E/E)\tan\theta_B$. In our case, we obtain $(\Delta E/E) = 3.4 \times 10^{-4}$. As a consequence, the incoherent broadening of the beam in the slit region due to the nonmonochromaticity upon reflection from the monochromator is equal to 635 mm × 0.18 × 3.4 × 10^{-4} = 0.04 mm. Therefore, the radiation nonmonochromaticity is insignificant when the slit is almost uniformly illuminated by an incoherent superposition of narrow coherent beams due to the relatively large size of the source. Hence, it is necessary to provide a constancy of the lattice parameter across the entire width of the slit. Otherwise, the rocking curve is broadened even in the case of instantaneous (stroboscopic) measurements [5].

In closing, let us consider practical applications of the method based on a dynamic variation in the lattice parameter of crystals in X-ray diffraction experiments. We can propose a few variants. First, the experimental results provide direct information on the degree of strain of the crystal in the case where ultrasound is generated by different methods. For example, it is possible to determine the character and intensity of spurious harmonics with shorter wavelengths. Furthermore, the maximum strain in the sample can be revealed when signals are fed with a specified power to the piezoelectric resonator. Second, the dynamic variation in the lattice parameter of the crystal makes it possible to control characteristics of the reflected beam. In particular, if the crystal under investigation is not rotated, the intensity of the reflected beam becomes periodic in time. This property can be used in time-resolved experiments. If the slit ahead of the crystal is removed and a narrow slit bounding the source size is placed, the beam whose spatial location varies with time due to a variation in the Bragg angle can be obtained in a dispersion scheme of the experiment. In this case, it is necessary to use broadband radiation, for example, from a synchrotron radiation source.

ACKNOWLEDGMENTS

We would like to thank V.V. Lider for his assistance in performing the experiments and for many pieces of helpful advice.

This study was supported by the Russian Foundation for Basic Research, project nos. 04-02-17363 and 06-02-08117.

REFERENCES

1. I. R. Éntin, Pis'ma Zh. Éksp. Teor. Fiz. **26** (5), 392 (1977) [JETP Lett. **26** (5), 269 (1977)].
2. A. R. Mkrtchan, M. A. Navasardyan, and V. K. Mirzoyan, Pis'ma Zh. Tekh. Fiz. **8**, 677 (1982) [Sov. Tech. Phys. Lett. **8** (6), 294 (1982)].
3. R. Tucoulou, D. V. Roshupkin, O. Mathon, et al., J. Synchrotron Radiat. **5**, 1357 (1998).
4. E. Zolotoyabko and J. P. Quintana, Rev. Sci. Instrum. **75**, 699 (2004).
5. A. E. Blagov, M. V. Koval'chuk, V. G. Kohn, et al., Zh. Éksp. Teor. Fiz. **128** (5), (2005) [JETP **101** (5), 770 (2005)].
6. M. V. Koval'chuk, É. K. Kov'ev, and E. G. Pinsker, Kristallografiya **20** (1), 142 (1975) [Sov. Phys. Crystallogr. **20** (1), 81 (1975)].
7. http://sergey.gmca.aps.anl.gov.

Translated by O. Borovik-Romanova